

## Origin of stick-slip motion in a driven two-wave potential

M. G. Rozman\*

*NORDITA, Blegdamsvej 17, DK-2100 Copenhagen Ø, Denmark*

M. Urbakh and J. Klafter

*School of Chemistry, Tel Aviv University, Tel Aviv 69978, Israel*

(Received 16 May 1996)

A model is presented of a particle that interacts with two periodic potentials, representing two confining plates, one of which is externally driven. The model leads to a spectrum of rich behaviors in the motion of the top driven plate: a stick-slip, intermittent kinetic regime, characterized by force fluctuations, and two types of sliding above a critical driving velocity  $v_c$ . Similar behaviors are typical of a broad range of systems including thin sheared liquids. A detailed analysis of the different regimes displays an interesting transition range between stick-slip and kinetic motion,  $\omega^{-2}$  power spectra of the force over a wide range of velocities below  $v_c$ , and a decrease of the force fluctuations that follows  $(v_c - v)^{1/2}$  for  $v < v_c$ . The velocity-dependent Liapunov exponents demonstrate that stick-slip dynamics is characterized by chaotic behavior of the top plate and the embedded particle. An equation is derived that provides a coarse-grained description of the plate motion near  $v_c$ . [S1063-651X(96)01511-5]

PACS number(s): 68.15.+e, 46.30.Pa, 05.45.+b, 05.40.+j

### I. INTRODUCTION

Stick-slip behavior has been observed in a variety of driven dissipative systems, such as charge- and spin-density waves [1], granular materials [2], earthquake faults [3], and systems of dry [4–7] and lubricated friction [8–11]. Stick-slip behavior has been also obtained in direct molecular-dynamical simulations [12–14]. Both experiments and theory show that stick-slip motion is accompanied by phenomena such as intermittent stick-slip, sliding, and force fluctuations. Sheared liquids confined between two atomically smooth parallel solid surfaces provide a good example where such a spectrum of behaviors can be observed in experiments [8,9] and in computer simulations [12–14]. Different models have been proposed to account for this type of motion in confined liquids including spring-block models [3] and chain or layer motion on a substrate [15,16].

In spite of growing interest, there is still relatively little understanding of the generic features of stick-slip dynamics. The origin of stick-slip motion and its related phenomena remains therefore still under some debate. For example, in the case of molecularly thin liquid films, molecular-dynamics simulations [12–14] suggest that a first-order phase transition between solidlike and liquidlike phases is responsible for the stick-slip behavior. A phenomenological model describing shear-induced melting during the transition from stick to slip has been considered recently [17,18]. In another example, of dry friction measurements [5], erratic stick-slip motion is claimed to be a manifestation of self-organized criticality [19], a concept that has been applied recently in the context of friction (see [20] for review).

In this paper we investigate a model of a single particle that interacts with two corrugated plates, one of which is

externally driven [21]. This simple minimalistic model does not show self-organized criticality or any phase transitions, but still manifests typical features of dry and lubricated frictional dynamics. Unlike previous models such as the Burridge-Knopoff model [3], train models [22], and the Frenkel-Kontorova-Tomlinson model [20,23] in our model we introduce a driving force on the top plate that mimics experimental conditions. The use of a single-particle model allows a detailed study of the system dynamics, which is more difficult within the frameworks of realistic models.

The present paper is organized as follows. In Sec. II we define the model and introduce the equations of motion. Section III presents results of numerical calculations. Different dynamical regimes are discussed and the transitions between them are analyzed. In Sec. IV we introduce an approximate description of the system's dynamics based on separation of "slow" and "fast" motions. Section V summarizes our results. In Appendix A we describe an algorithm for the calculation of the Liapunov exponents. In Appendix B equations describing the motion of the top plate averaged over fast oscillations are derived and solved. Appendix C presents a stability analysis of the regimes of motion.

### II. THE MODEL

Consider a one-dimensional model that includes two rigid plates and a single particle of mass  $m$  embedded between them. The interaction between the particle and each of the plates is described by a periodic potential  $U(x)$ . There is no direct interaction between the plates. The top plate of mass  $M$  is pulled by a linear spring with force constant  $K$  connected to a stage that moves with a velocity  $v$  (see Fig. 1 for a sketch of the model).

The coupled equations of motion for the top plate and the particle are

---

\*Permanent address: Institute of Physics, Riia 142, EE2400 Tartu, Estonia.

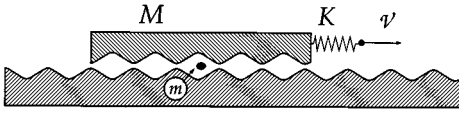


FIG. 1. Schematic sketch of a model geometry.

$$M\ddot{X} + \eta(\dot{X} - \dot{x}) + K(X - \mathcal{V}t) + \frac{\partial U(x-X)}{\partial X} = 0, \quad (1a)$$

$$m\ddot{x} + \eta\dot{x} + \eta(\dot{x} - \dot{X}) + \frac{\partial U(x)}{\partial x} + \frac{\partial U(x-X)}{\partial x} = 0, \quad (1b)$$

where  $x$  and  $X$  are the coordinates of particle and the top plate, respectively. The second term in Eq. (1a) and the second and the third terms in Eq. (1b) describe the dissipative forces between the particle and the plates and are proportional to their relative velocities. These terms account for dissipation due to phonons and/or other excitations. The third term in Eq. (1a) is the driving force due to the stage motion. The remaining terms are due to the spatially periodic potential interaction between the particle and the plates.

Within our model the frictional force acting on the top plate is determined by the particle-plate interaction and is equal to

$$F = -\frac{\partial U(x-X)}{\partial X} - \eta(\dot{X} - \dot{x}). \quad (2)$$

The first term is the potential component of the frictional force and the second one describes the dissipative contribution. We choose the potential  $U(x)$  to be

$$U(x) = -U_0 \cos\left(\frac{2\pi}{b}x\right). \quad (3)$$

When the top plate moves infinitely slowly, the particle follows adiabatically the motion of the plate. In this case the resistance force is  $F = (2\pi/b)U_0 \sin(2\pi f/b)$ , where  $f$  is the relative displacement of the periodic potentials that correspond to the top and bottom plates. The maximum value of this force can be interpreted as the static frictional force

$$F_s = \frac{2\pi U_0}{b}. \quad (4)$$

This force is the smallest driving force for which no stationary states exist.

In the present paper we focus on the dynamical behavior of the top plate and of the particle as the driving velocity of the stage is varied. It is convenient to introduce dimensionless space and time coordinates  $y = x/b$ ,  $Y = X/b$ , and  $\tau = t\omega$ , where  $b$  is the period of the corrugation represented by the potential  $U(x)$  and  $\omega = (2\pi/b)\sqrt{U_0/m}$  is the frequency of the small oscillations of the particle in the minima of potential. Equations (1) can be rewritten then in a dimensionless form as

$$\ddot{Y} + \epsilon\gamma(\dot{Y} - \dot{y}) + \alpha^2(Y - v\tau) - \frac{\epsilon}{2\pi}\sin[2\pi(y - Y)] = 0, \quad (5a)$$

$$\ddot{y} + \gamma(2\dot{y} - \dot{Y}) + \frac{1}{2\pi}\sin(2\pi y) + \frac{1}{2\pi}\sin[2\pi(y - Y)] = 0, \quad (5b)$$

where  $\gamma = \eta/(m\omega)$  is a dimensionless friction constant,  $\epsilon = m/M$  is the ratio of particle and plate masses,  $\alpha = \Omega/\omega$  is the ratio of frequencies of the free oscillations of the top plate  $\Omega = \sqrt{K/M}$  and the particle, and  $v = \mathcal{V}/(\omega b)$  is the dimensionless stage velocity. Here one distinguishes between the underdamped and overdamped limits. We concentrate on the underdamped case. Equations (5) relate to the problem of friction in lubricating films [24,15,13] and in the limit  $\alpha \rightarrow \infty$  reduce to the problems of a particle in a two-wave potential [25,26] and of a parametric oscillator [27], both actively studied in the theory of nonlinear dynamical systems.

### III. RESULTS OF SIMULATIONS

Our simulations demonstrate that, this model of a single particle in a driven two-wave potential is rich in transitions among different dynamical behaviors. We have observed four different dynamical regimes [28]: (a) at low velocities we observe a stick-slip motion of the plate, (b) as the stage velocity increases the motion of the top plate is characterized by irregular stop events with time intervals between them that increase rapidly with  $v$  and the stick-slip motion becomes more erratic and intermittent, (c) in the kinetic regime the top plate never stops and the spring executes chaotic oscillations, and (d) smooth sliding occurs when the stage velocity is above the critical velocity  $v_c$ . Figure 2 illustrates the time dependence of the spring force  $-K(X - \mathcal{V}t)$  and of the particle velocity in these typical regimes. Here we concentrate on the dynamics of the system under the condition  $\alpha = \Omega/\omega \ll 1$ . In the calculations reported below we use parameter values that belong to the underdamped case:  $\alpha = 0.02$ ,  $\gamma = 0.1$ , and  $\epsilon = 0.125$ , which lead to the following regimes.

#### A. Regimes of motion

(a) *Stick-slip motion.* The motion of the top plate in the first regime [see Fig. 2(a)] is typical of relaxation oscillations. The top plate is initially at rest and the spring connecting it to the stage stretches linearly in time. When the force on the plate exceeds the static frictional force  $F_s$  [Eq. (4)] the top plate begins to slide. Since the frictional force in this kinetic state is less than  $F_s$ , the plate accelerates. Owing to the inertia, the velocity of the plate  $\dot{Y}$  is initially lower than the driving velocity  $v$  and the spring will continue to extend until finally  $\dot{Y} > v$ . The maximum spring force will therefore be greater than  $F_s$ . When the plate velocity is  $\dot{Y} > v$  the spring force decreases until it reaches some value where the motion stops and then the process repeats. Stopping of the top plate during every period of the spring force oscillations is the characteristic feature of the first regime. As a result, the plate motion is determined by the interplay between static and kinetic friction.

It should be noted that the stick-slip motion is periodic only for very low stage velocities  $v < v_0$ , where  $v_0 = 0.03$  for the above values of the parameters  $\alpha, \gamma, \epsilon$ . For higher veloci-

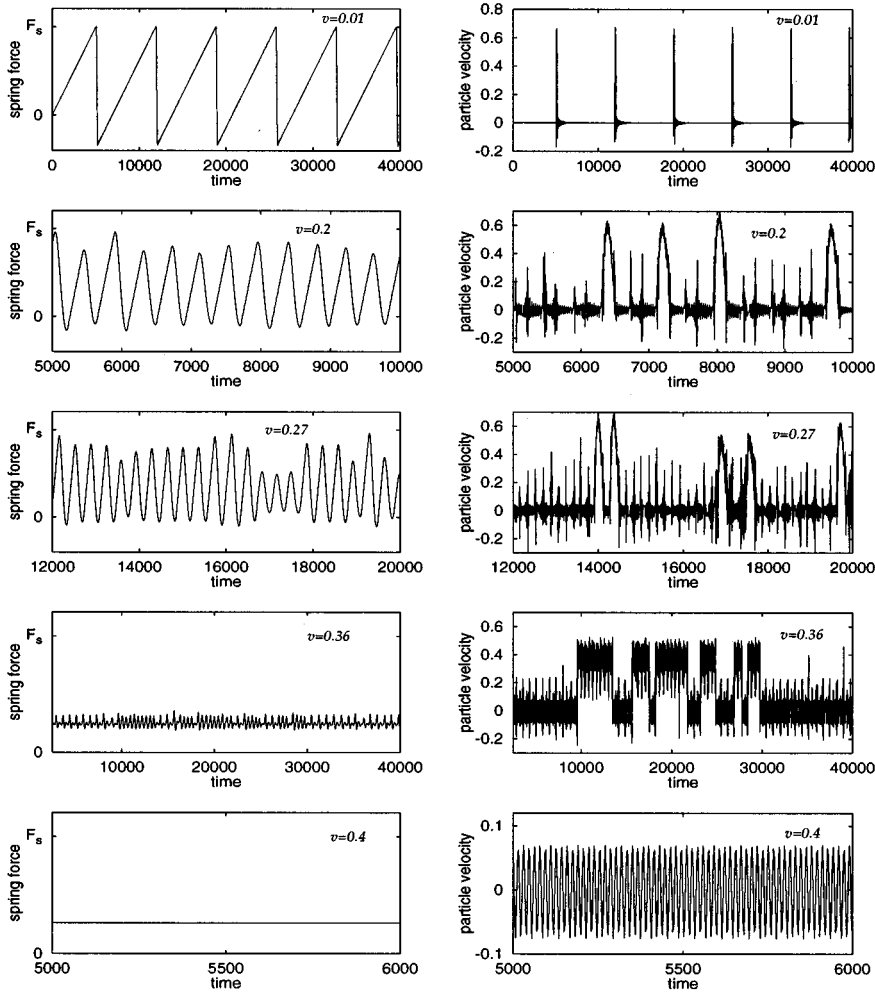


FIG. 2. Different regimes of the particle and the plate motion. Left column, the spring force versus time; right column, the particle velocities versus time. Stage velocities are denoted on the graphs.

ties, still within regime (a), weak fluctuations of the amplitude and of the period of the spring force oscillations have been observed. For  $v > v_0$  the trajectories of the top plate and the particle are sensitive to initial conditions, which is a manifestation of the chaotic nature of the system. The transition from periodic to chaotic stick-slip motion occurs through a sequence of period-doubling bifurcations and chaotic windows and depends on the mass of the top plate and on the spring constant.

In order to provide a quantitative measure of the degree of stochasticity of the motion we have calculated the velocity dependence of the largest Liapunov exponent of the trajectories (see Fig. 3). In regime (a) this exponent is negative only for  $v < v_0$ , supporting the periodicity of the motion. In this range of velocities the system (the particle and the top plate) has time to relax to the ground state after sliding. For higher velocities the largest Liapunov exponent becomes positive and increases slowly with the driving velocity. This points towards a rise in the dynamical chaos with the increase of  $v$ . It should be mentioned that Liapunov exponents can be extracted from experimental data of the time dependence of the spring force or the velocity of the top plate [29]. A method for calculating the Liapunov exponents is outlined in Appendix A.

We have also noticed that at low stage velocities the amplitude of the spring force depends only slightly on  $v$  and the period of oscillations decreases with the increase of  $v$ . In this

range of velocities the time-averaged velocity and the displacement of the particle are much smaller than the average velocity and the displacement of the top plate.

(b) *Intermittent stick-slip motion.* For higher stage velocity the top plate does not necessarily stop during the spring oscillations and the motion becomes more erratic [see Fig. 2(b)]. These higher velocities correspond therefore to a transition regime between the stick-slip and kinetic regimes. In order to define this transition quantitatively we introduce the

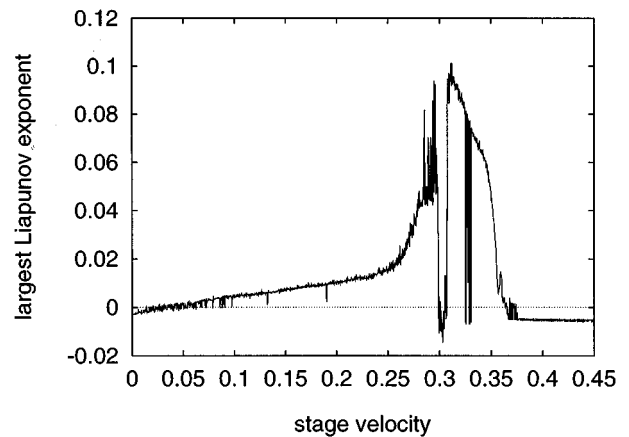


FIG. 3. Velocity dependence of the largest Liapunov exponent.

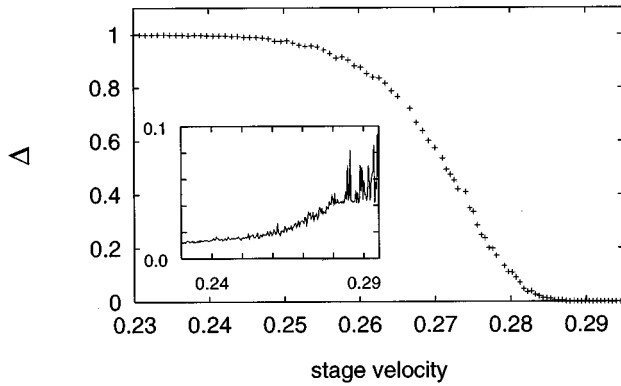


FIG. 4.  $\Delta$  versus stage velocity in the intermittent regime. The inset shows the largest Liapunov exponent in the same velocity range.

parameter  $\Delta = T_s/T$ , where  $T_s$  is the net time during which the spring force oscillations are accompanied by stopping of the top plate and  $T$  is the total time of simulations. Namely,  $\Delta$  measures how much time the plate spends in stick-slip motion relative to the total time, which includes kinetic segments. Figure 4 presents  $\Delta$  as a function of the stage velocity. The parameter  $\Delta$  changes from  $\Delta=1$  (complete stick-slip motion) to  $\Delta=0$  (kinetic motion) within a narrow velocity interval that separates the stick-slip and kinetic regimes. This velocity interval, where  $0 < \Delta < 1$ , can be defined naturally as an intermittent regime. The calculation of the parameter  $\Delta$  allows us to introduce a well-defined boundary at  $v=v_k$  (where  $\Delta=0$ ), between the intermittent and kinetic regimes. It should be noted that the value of the largest Liapunov exponent grows rapidly in this intermittent regime (see inset to Fig. 4), showing an increase of the dynamical chaos in the system.

(c) *Kinetic regime.* In the kinetic regime where the top plate never stops (Fig. 2) the amplitude of the spring force strongly depends on the stage velocity  $v$ . Here the frictional force is less than the static friction for all times and the time-averaged velocity and displacement of the particle are close to half of those of the top plate. As we discuss below, the nature of the motion in this regime is determined by an

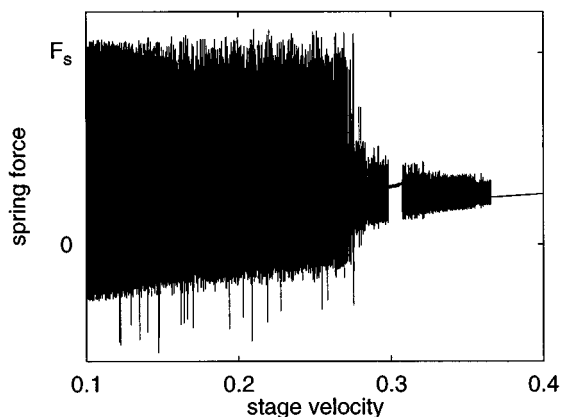


FIG. 5. Time oscillations of the spring force for the stage moving with a small constant acceleration. For convenience the stage velocity (instead of time) is indicated on the axis.

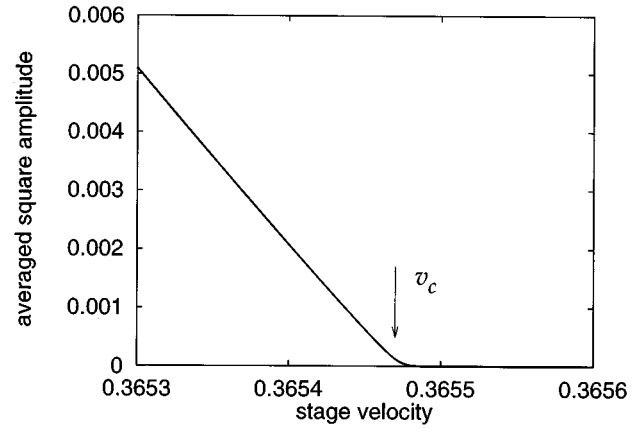


FIG. 6. Variance of the oscillation near  $v_c$ . The deviation of the graph from the straight line in the nearest vicinity of  $v_c$  is connected with the divergence of the relaxation time as  $v$  approaches  $v_c$ , as discussed in the text.

effective velocity-dependent friction force. As the stage velocity is varied within this regime, the trajectories of the particle show that the particle jumps between the two plates. It clings to each of them for times much longer than the characteristic modulation time induced by the stage motion (natural period)  $1/v$ . In Fig. 5 we note that windows of sliding motion appear within the kinetic region. Here the spring force is plotted versus a stage velocity that increases with a small constant acceleration. The number and widths of the windows depend on the mass of the top plate, the spring constant, and friction constant  $\eta$ . In these velocity windows the largest Liapunov exponent is negative (Fig. 3), which is consistent with the nonchaotic character of smooth sliding.

(d) *Sliding regime.* A sharp boundary at  $v=v_c$  is observed between the kinetic and sliding regimes. When the velocity approaches the critical velocity  $v_c$  from below, the root mean square of the time oscillations of the spring force decreases as  $\sqrt{v_c-v}$  and sliding sets in. Figure 6 displays the variance of the oscillation amplitude, which behaves as  $v_c-v$  for  $v < v_c$ .

In the sliding regime the spring force performs ‘‘microscopic’’ oscillations with a period of the order  $1/v$  and with amplitudes much smaller than in regimes (a) and (b). The time-averaged frictional force is proportional to the stage velocity (the single-particle ‘‘analog’’ of a liquid phase between two plates).

The velocity dependence of the Liapunov exponent gives a clear manifestation of the transition to sliding. As the stage velocity increases and approaches  $v_c$ , the largest Liapunov exponent decreases steeply and becomes negative at  $v=v_c$ , suggesting the disappearance of chaos in the transition. This concurs with the reduction in the amplitude of the spring force oscillations.

Under the condition  $\Omega \ll \omega$  assumed in this paper, we have found a very weak dependence of  $v_c$  on the mass of the top plate  $M$  and on the spring constant  $K$ . For  $v_c < v < v_{th}$ , where  $v_{th}=1.3$  for our choice of parameters, the particle does not jump between the two plates but rather clings to one of them and oscillates within one spatial period of the corrugated potential  $U(x)$ . At higher stage velocities  $v > v_{th}$ , the character of sliding changes. The particle ceases to feel the

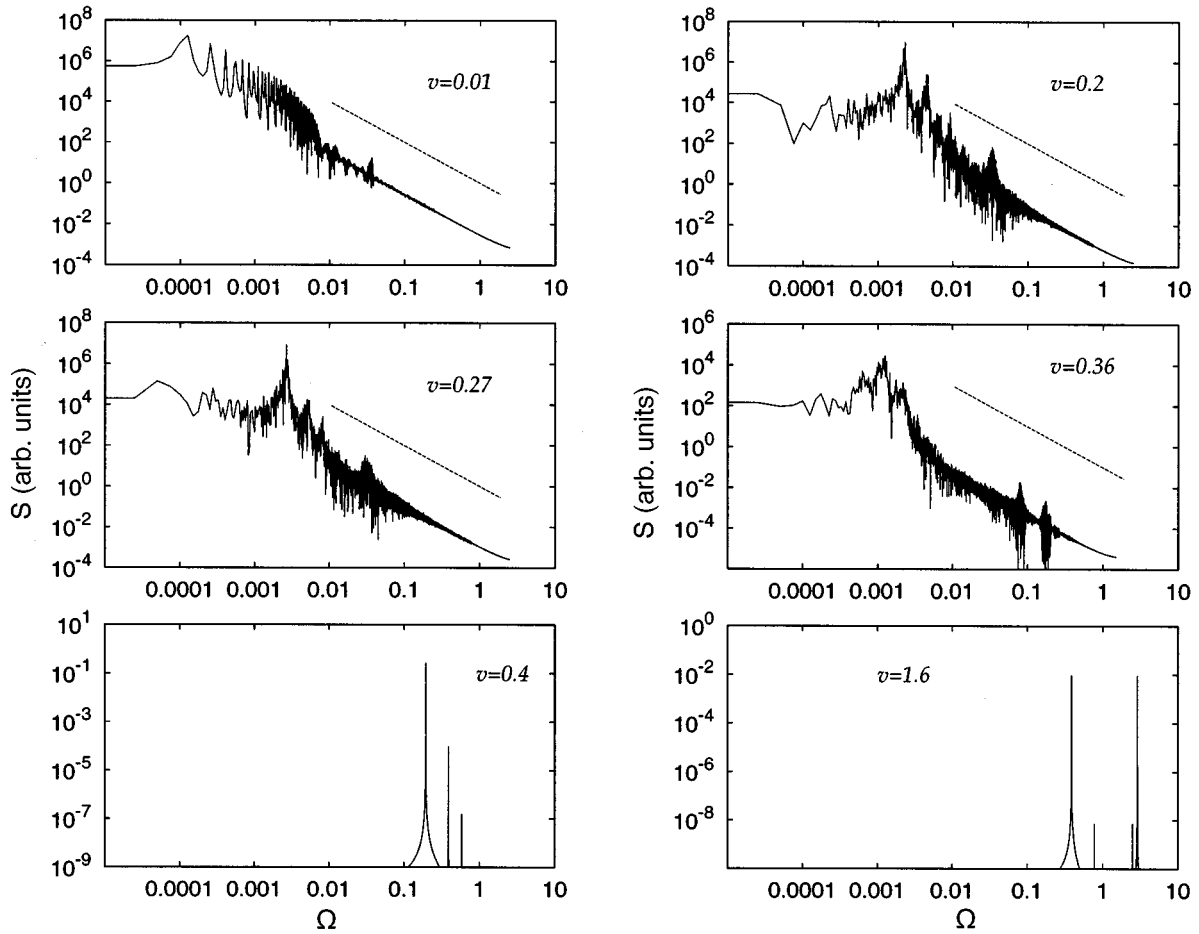


FIG. 7. Power spectra of spring force fluctuations (in log-log scale) for different regimes of motion. The dotted line of slope  $-2$  is provided for reference.

corrugation of the plates and moves with the velocity  $v/2$ . The frictional force becomes the same as for flat plates. This change of the sliding state is accompanied by the drop of the frictional force and can be interpreted as the analog effect of shear thinning [30,31].

### B. Power spectra

We have also calculated the power spectra  $S(\omega)$  of the spring force and of the velocities of the top plate and the particle for the whole range of the stage velocities. Here we discuss the power spectra of the spring force only (Fig. 7). The power spectra  $S(\omega)$  depend on the stage velocity and for  $v < v_c$  a power-law behavior  $S(\omega) \sim \omega^{-2}$  for frequencies  $\omega$  above some cutoff is observed. For small driving velocities ( $v=0.01$  on Fig. 7), when the motion of the top plate looks like relaxation oscillations, this power law can be observed also in the low-frequency domain. The origin of  $\omega^{-2}$  frequency dependence are abrupt drops of the spring force typical of relaxation oscillations. Power spectra with the  $\omega^{-2}$  tails were observed in real systems that demonstrate stick-slip motion [7,24].

As discussed earlier, the time-dependent spring force evolves from periodic to erratic behavior as the stage velocity  $v$  increases. This leaves the power law unchanged but introduces large fluctuations as we move from low velocities

towards  $v_c$ . The noisy  $\omega^{-2}$  behavior extends over a few orders of magnitude in  $S(\omega)$  and  $\omega$ . When sliding prevails the power spectra exhibit well defined dominating frequencies that originate from the motion of the periodic potential with velocity  $v$  (Fig. 7,  $v=0.4, 1.6$ ).

### C. Hysteresis

Another interesting property amenable to experimental tests is the hysteretic behavior of the spring force as the stage velocity changes. In order to investigate this phenomenon we have carried out calculations for the case where the stage moves with a small constant acceleration. Figure 8 shows the time dependence of the spring force for positive and negative accelerations  $a$ . For convenience the  $x$  axis shows the velocity of the stage at time  $t$ . The hysteresis shown in Fig. 8 reflects the coexistence of two dynamical states in the vicinity of  $v_c$ : one corresponds to a kinetic stick-slip motion and another corresponds to smooth sliding. The figure shows also the envelope of the time dependence of the spring force found within the analytical theory that is discussed in Sec. IV and in Appendix B. The envelope has the square-root behavior near  $v_c$  that concurs with the velocity dependence of the time-averaged amplitude of the spring force shown in Fig. 6. It should be mentioned that the transient time required to reach the stationary state diverges at  $v=v_c$ . The approxi-

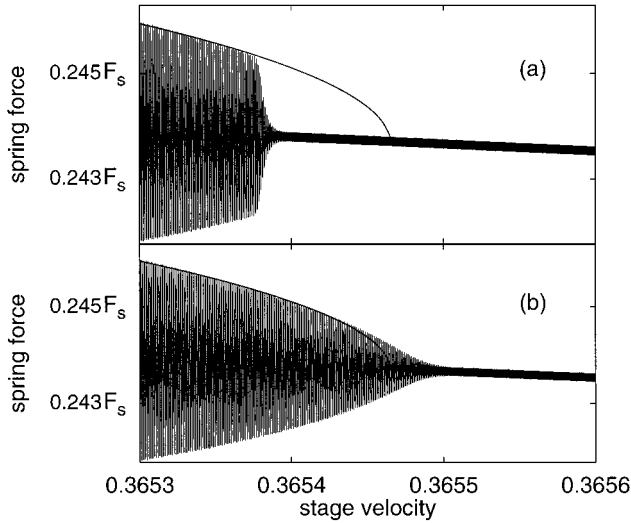


FIG. 8. Hysteretic behavior of spring force near  $v_c$ . The top figure corresponds to the motion of the driving stage with a small negative acceleration  $a < 0$ , the bottom figure corresponds to a positive acceleration  $a > 0$ .

mate analytical solution discussed in Appendix B predicts that the transient time diverges as  $1/|v - v_c|$ . The divergence of the transient time at  $v = v_c$  leads to the deviation of the envelope from the square-root law in the immediate vicinity of  $v_c$ , emphasizing that caution has to be taken when numerical calculations are carried out in this region.

#### IV. ADIABATIC APPROXIMATION AND CRITICAL VELOCITY

It is possible to give an analytical description of the motion of the top plate connected to the spring that predicts the transition at  $v_c$ . We introduce two assumptions for the top plate dynamics in the vicinity of  $v_c$ : (a) the characteristic frequency of the large-scale plate motion is much smaller than both the characteristic frequency of the particle oscillations and the natural frequency  $\nu$  and (b) the mass of the particle is smaller than the mass of the top plate, i.e.,  $\epsilon < 1$ . Hence the top plate and the particle display “slow” and “fast” motions and there is a separation of time scales; namely, the adiabatic approximation prevails. Under these assumptions we solve Eqs. (5). For Eq. (5b) we assume that the plate moves with a constant velocity  $\dot{Y} = V$ . For the particle motion we get

$$\ddot{y} + \gamma(2\dot{y} - V) + \frac{1}{2\pi}\sin(2\pi y) + \frac{1}{2\pi}\sin[2\pi(y - V\tau)] = 0. \quad (6)$$

Equation (6) has been used to describe a dissipative parametrically driven pendulum and a dissipative motion of a particle in two waves. In spite of its apparent simplicity, Eq. (6) is not integrable and leads to a rich spectrum of phenomena (see [25–27] and references therein).

The solutions of Eq. (6),  $y(\tau, \dot{Y})$ , depend parametrically on  $\dot{Y}$ . Substituting  $y(\tau, \dot{Y})$  into Eq. (5a) we get

$$\ddot{Y} - \epsilon F(\tau, Y, \dot{Y}) + \alpha^2(Y - v\tau) = 0, \quad (7)$$

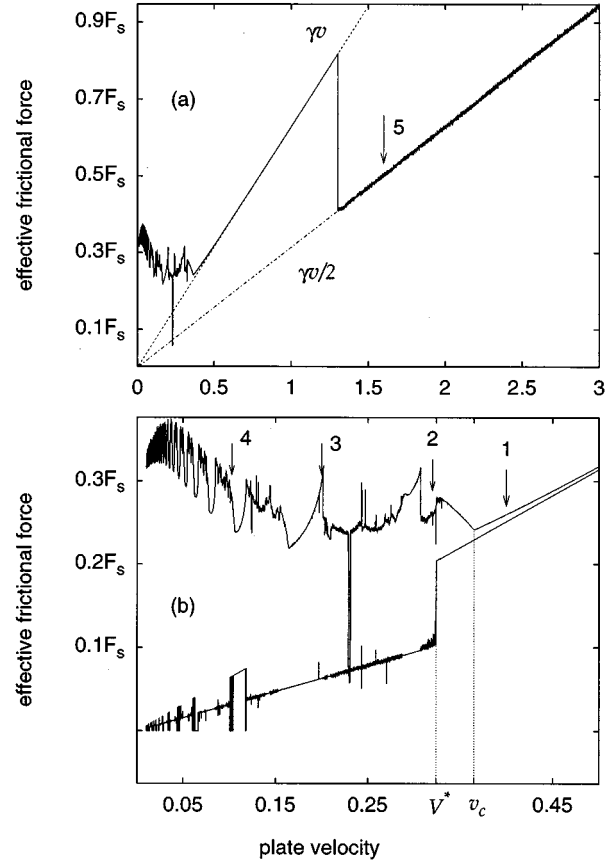


FIG. 9. Friction forces acting on the top plate as function of plate velocity. (a) General view. (b) Small velocities. The lower curve is the dissipative contribution; the upper curve is the net force. The arrows indicate velocities of the plate corresponding to particle trajectories shown in Fig. 10.-

where the dimensionless particle-plate interaction force

$$F(\tau, Y, \dot{Y}) = \frac{1}{2\pi} \sin[2\pi(y - Y)] - \gamma(\dot{Y} - \dot{y}) \quad (8)$$

contains fast-oscillating components. Averaging Eqs. (7) and (8) over the fast oscillations, we obtain an equation for the slow oscillating component of the spring length  $L(\tau) = Y(\tau) - v\tau$ ,

$$\ddot{L} - \epsilon \phi(\dot{L} + v) + \alpha^2 L = 0, \quad (9)$$

where the time-averaged force  $\phi(\dot{Y}) = \langle F(\tau, Y, \dot{Y}) \rangle$  depends only on the velocity of the plate and presents the effective friction for the plate motion.

Before we solve Eq. (9) we discuss the velocity dependence of the time-averaged force  $\phi(\dot{Y})$ , given by the averaged Eq. (8), that contains two terms [see also Eq. (2)]. The first one is the potential component of the frictional force and the second one describes the dissipative contribution (see Fig. 9). The structure in the velocity dependence of  $\phi(\dot{Y})$  in the figure corresponds to different types of particle trajectories (Fig. 10). We see that the motion of the particle has three characteristic behaviors: at low velocities  $V < V^*$ , the average velocity of the particle predominantly is equal to  $\frac{1}{2}V$ ,

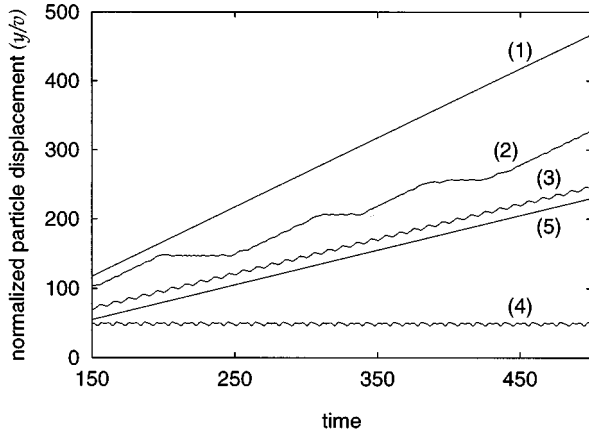


FIG. 10. Particle trajectories for selected values of the plate velocities.

except for short windows where the particle is trapped by one of the plates; for  $V^* < V < v_{th}$  the particle always clings to one of the plates; and for  $V > v_{th}$  the particle motion with the velocity  $V/2$  becomes stable. This is illustrated clearly by the dissipative component of the frictional force presented in Fig. 9.

There are three types of the particle trajectories for  $V < V^*$ : (i) the particle jumps between two plates being trapped by each of them for the time much longer than  $V^{-1}$  (curve 2 in Fig. 10); (ii) the particle undergoes fast oscillations with the period  $V^{-1}$ , around the trajectory  $x = \frac{1}{2} Vt$  (curve 3 in Fig. 10); and (iii) the particle clings to one of the plates (curve 4 in Fig. 9). In the first two cases the time-averaged velocity of the particle is equal to  $\frac{1}{2}V$  and in the third case it equals  $V$  or  $0$ . The dissipative component of the friction (lower curve in Fig. 9) reflects clearly these features of the motion. The local minima and maxima in the velocity dependence of the net frictional force shown in Fig. 9 correspond to the trajectories of the types (3) and (4). It should be stressed that for all trajectories in the region  $V < V^*$  (except for  $V=0.23$ , which corresponds to a stable motion of the particle with the velocity  $\frac{1}{2}V$ ) the fluctuations of the particle velocity are of the order of, or even larger than, the velocity of the top plate. Curve 1 in Fig. 10 describes the case  $V > V^*$ .

The velocity-dependent features described above are similar to those discussed within our original model. Note that the transition velocity  $V^*$  found in the reduced model is somewhat smaller than the previously determined critical velocity  $v_c$ . However, motion with small fluctuations in the particle velocity occurs only for  $V > v_c$ . In spite of the particle being trapped by one of the plates in the region  $V^* < V < v_c$ , the fluctuations of the velocity are large, being of the order of  $V$ . The fluctuations decrease when we approach  $v_c$  from below. The decay of the potential component of the frictional force in the region  $V^* < V < v_c$ , which is proportional to the square of the amplitude of the velocity fluctuations, manifests the transition from erratic to smooth sliding. The sharp decrease of the potential component of the effective friction corresponds to the disappearance of global chaos in the dynamics of the particle.

At higher plate velocities  $V > v_{th}$  the character of the particle motion changes again and the trajectory  $x = \frac{1}{2}Vt$  becomes stable (curve 5 in Fig. 10). Here the characteristic frequency of the particle motion is smaller than the modulation frequency induced by the plate motion  $V$  and the particle cannot respond to the variation of the plate-particle interaction. The frictional force that is  $\eta V$  for  $v_c < V < v_{th}$  changes to  $\eta V/2$  for  $V > v_{th}$ . The latter behavior corresponds to effectively flat plates.

We now return to the discussion of the solution of Eq. (9) in the vicinity of the critical velocity  $v_c$ . The important feature of the frictional force  $\phi(v)$  in Eq. (9), is the presence of a single minimum in the considered velocity range (see Fig. 9). For stage velocities  $v < v_c$  Eq. (9) has solutions that correspond to an oscillating spring force (limit cycle). For  $v > v_c$  it has a static solution (fixed point) that describes the sliding regime. An analytical solution of Eq. (9), asymptotic in the small parameter  $\epsilon$ , can be obtained using Bogoliubov-Krylov technique [32] (see Appendix B). One obtains that the critical velocity coincides with the position of the minimum of the effective friction force. The value of the critical velocity found from the adiabatic approximation Eq. (9) agrees well with the results of the numerical analysis of Eqs. (5). For velocities slightly less than  $v_c$  the amplitude of the force oscillations really scale as  $L \sim \sqrt{v_c - v}$ , as observed numerically (Fig. 6).

The above considerations demonstrate that the adiabatic approach describes reasonably well the dynamics of the top plate when the driving velocity is close to  $v_c$ . Within this picture the presence of velocity intervals where the friction force decreases with increasing velocity is a crucial condition for the existence of force fluctuations. It should be mentioned that Eq. (9) does not account for the chaotic character of the motion, but correctly describes the amplitudes of force oscillations.

## V. DISCUSSION

To summarize, a single-particle model has been proposed that displays the dynamical features resembling experimental and simulation results obtained for nanoscale liquid films under shear. The model leads to stick-slip motion, the kinetic regime, and the transition to sliding at a critical velocity  $v_c$ . For a wide range of system parameters we find that the motion is chaotic, as supported by calculated Liapunov exponents. Our calculations suggest that the information obtained following the macroscopic motion of a plate does not allow one to draw an unambiguous conclusion on the dynamical structure of a molecular system embedded between the plates.

It should be emphasized that characteristic to our model is one frequency  $\omega$ , which is related to the particle-plate interaction. This of course determines the different transition frequencies we obtain; for instance, the transition to sliding occurs at  $v_c \sim \omega b$ . Adding more interacting particles towards a bulk liquid description will introduce other characteristic frequencies that will compete with  $\omega$ . This will be investigated in our future work, where we consider a chain embedded between the two plates.

We believe that although the model is only a single-particle picture, some of the predictions may hold for larger

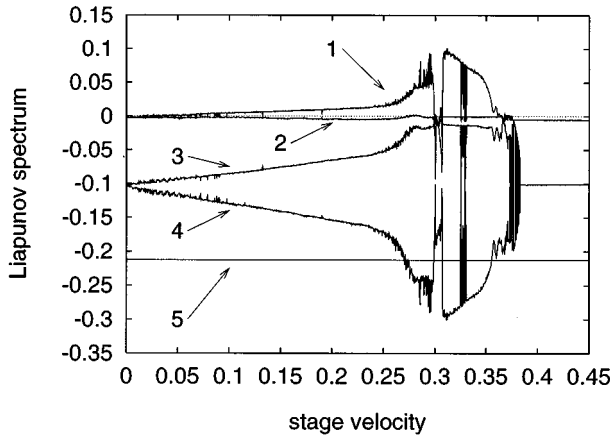


FIG. 11. Liapunov spectrum. Curves 1–4 show the dependence of Liapunov exponents on the stage velocity. Line 5 shows the control sum (A1).

systems and are amenable to experimental verification: the power spectra of the force fluctuations in the different regions, the decrease of the force amplitude fluctuations in the vicinity of  $v_c$ , which in our model follows  $(v_c - v)^{1/2}$ , hysteretic behavior, and an analysis of the time dependence of the force in terms of Liapunov exponents. The chaotic behavior observed suggests that the use of recently proposed chaos-controlling approaches is possible in order to convert chaos into periodic motion.

**ACKNOWLEDGMENTS**

We thank Yuri Braiman for his thoughtful comments and J. M. Drake for fruitful discussion. Financial support for this work by the Israel Science Foundation, administered by the Israel Academy of Science and Humanities, is gratefully acknowledged. M.R. acknowledges the support of the Alexander von Humboldt Stiftung and the Estonian Science Foundation under Grant No. 350.

**APPENDIX A: NUMERICAL EVALUATION OF LIAPUNOV EXPONENTS**

Liapunov exponents are the averaged exponential rates of divergence or convergence of nearby orbits in phase space. Any system with at least one positive exponent is defined to be chaotic [33,34]. The magnitude of the exponent reflects the time scale over which the system dynamics becomes unpredictable and provides a quantitative measure of the degree of stochasticity of a trajectory of the system.

A technique for numerical determination of a complete Liapunov spectrum from a set of differential equations has been developed in [35,36]. (See also [34] for a review.) In order to achieve a reasonable precision in the calculation of the exponents, one needs to perform a long-time averaging along a trajectory. In our calculations the following property of the Liapunov spectrum of the system (5) has been used for the control of convergence:

$$\sum_{i=1}^4 \lambda_i = -\gamma(2 + \epsilon). \tag{A1}$$

The calculated Liapunov spectrum and the control sum (10) are presented in Fig. 11.

**APPENDIX B: ANALYTICAL SOLUTIONS**

In this appendix we present the asymptotic (in the small parameter  $\epsilon$ ) solution of Eq. (9) in the vicinity of  $v_c$ . The solution of Eq. (9) for  $\epsilon=0$  is

$$L = r \cos \psi,$$

with a constant amplitude  $r$  and a uniformly rotating phase angle  $\psi$ ,

$$\dot{r} = 0, \quad \dot{\psi} = \omega.$$

For  $\epsilon \neq 0$  the nonlinear term results in the appearance of higher harmonics. We seek therefore the solution of Eq. (9) of the form [32]

$$L = r \cos \psi + \sum_n \epsilon^n u_n(r, \psi). \tag{B1}$$

Here  $u_n(r, \psi)$  are  $2\pi$ -periodic functions of the angle  $\psi$  and  $r(t)$  and  $\psi(t)$  are functions of time. In order to define these functions uniquely we assume that they do not include the fundamental harmonic, i.e.,  $r$  is the net amplitude of the fundamental harmonic of the oscillations.

Under the condition  $\epsilon \ll 1$  the term  $\epsilon \phi(v)$  is a small perturbation to the linear oscillator. To second order in  $\epsilon$  we get for the amplitude of the stick-slip motion

$$\dot{r} = \frac{\epsilon}{2} r \left( \frac{\partial \phi}{\partial v} + \frac{1}{8} \alpha^2 r^2 \frac{\partial^3 \phi}{\partial v^3} + \dots \right), \tag{B2}$$

where terms containing higher even-order powers of  $r$  and higher odd-order derivatives of  $\phi$  with respect to parameter  $v$  are neglected.

Let us consider the case where the effective friction force  $\phi(v)$  has a single minimum at a  $v = v_m$ , i.e.,

$$\left. \frac{\partial \phi(v)}{\partial v} \right|_{v=v_m} = 0, \tag{B3}$$

such that

$$\left. \frac{\partial^3 \phi(v)}{\partial v^3} \right|_{v=v_m} > 0. \tag{B4}$$

We also assume that the effective friction force  $\phi(v)$  is smooth enough so that higher derivatives are much smaller than (B4) and can be dropped in Eq. (B2) (this approximation does not describe hysteresis).

We note that the simplest functional form of  $\phi(v)$  satisfying Eqs. (B3) and (B4) is a cubic polynomial

$$\phi(v) = a + bv + cv^2 + dv^3.$$

Upon substituting this ‘‘minimal’’ form into Eq. (9) we get the Rayleigh equation.

Steady-state solutions of Eq. (B2) are

$$r=0, \quad (\text{B5})$$

$$r^2 = -8 \frac{d\phi}{dv} \frac{d^3\phi}{dv^3}. \quad (\text{B6})$$

The nontrivial solution of Eq. (B6) exists only for velocities smaller than the critical one  $v_m$  because  $d\phi/dv < 0$  only for  $v < v_m$ . The trivial solution Eq. (B5) that corresponds to the sliding-type motion of the plate exists for all velocities, but is stable only for velocities larger than  $v_m$ .

We conclude that the critical velocity  $v_c$ , which corresponds to the minimum of the effective frictional force, is  $v_c \equiv v_m$ . For velocities slightly less than the critical one the amplitude of the stick-slip motion calculated according to Eq. (B6) scales as

$$r \sim \sqrt{v_c - v}, \quad (\text{B7})$$

in agreement with the numerical simulations.

In order to consider transient regimes for  $v \sim v_c$  it is necessary to linearize Eq. (B2) near  $v_c$ . The solution of the linearized equation shows that the time required to achieve the steady-state solutions diverges as  $|v - v_c|^{-1}$  as  $v \rightarrow v_c$ .

### APPENDIX C: STABILITY OF SLIDING

In this appendix we present the results of a linear stability analysis of the sliding in the adiabatic approximation. We give an explanation of some features that appear in the friction force as presented on Fig. 9, namely, the deep narrow minimum at  $v = 0.23$  [Fig. 9(b)] and the abrupt drop accompanied by a change of the friction law asymptotics from  $\phi = \gamma v$  to  $\phi = \gamma v/2$  [Fig. 9(a)].

Equations (6) and (9) have an exact solution

$$y_s(\tau) = \frac{1}{2} v \tau, \quad (\text{C1})$$

$$\dot{L} = 0, \quad (\text{C2})$$

describing the sliding motion of the top plate  $\dot{Y} = v$  and steady drift of the particle  $\dot{y} = v/2$ . In order to investigate the

stability of the solution (C1) we study the general solution of Eq. (6) written as a sum of Eq. (C1) and a small deviation  $w(\tau)$ :

$$y = y_s(\tau) + w(\tau). \quad (\text{C3})$$

Substituting Eq. (C3) into Eq. (6), linearizing with respect to  $w$ , and introducing the notations

$$z = \frac{1}{2} v \tau, \quad \eta = \frac{4\gamma}{\pi v}, \quad q = \frac{4}{\pi^2 v^2}. \quad (\text{C4})$$

we get

$$\frac{d^2 w}{dz^2} + \eta \frac{dw}{dz} + 2q \cos(2z) w = 0. \quad (\text{C5})$$

Equation (C5) is the canonical form [37] of the Mathieu equation with an additional friction term.

The sliding solution (C1) is the stable solution of Eq. (6) if the solution of Mathieu equation (C5)  $w$  is bounded. The issue of the stability of sliding is therefore related to general results available on the Mathieu equation (see [37] and references therein). We finally conclude the following.

(a) For small and intermediate values of driving velocities, such that  $q \gg 1$ , there are only exponentially narrow velocity ranges where the sliding solution (C1) is stable. The deep minimum of the effective frictional force at  $v = 0.23$  [see Fig. 9(b)] is the manifestation of this kind of motion.

(b) For large values of the stage velocity, i.e., for sufficiently small values of the parameter  $q$  in (C5),  $q \ll 1$ , the sliding regime is always stable. The particle in this regime moves with the constant velocity  $v/2$ .

The above analysis does not describe all possible types of stable sliding. In particular, for driving velocities slightly above  $v_c$  the particle gets stuck to one of the plates and its motion therefore is not of type (C1), but rather  $y = v\tau$  or  $y = \text{const}$ . However, with the increase of stage velocity, the particle must abruptly change its velocity from  $v$  or  $0$  to  $v/2$ . This drop in the particle drift velocity is accompanied by a corresponding drop in the effective frictional force [see Fig. 9(a)] and by a change of friction law from  $\phi = \gamma v$  to  $\phi = \gamma v/2$ .

- 
- [1] G. Grüner, Rev. Mod. Phys. **60**, 1129 (1988).  
 [2] F. Radjai, P. Evesque, D. Bideau, and S. Roux, Phys. Rev. E **52**, 5555 (1995).  
 [3] J. M. Carlson, J. S. Langer, and B. E. Shaw, Rev. Mod. Phys. **66**, 657 (1994).  
 [4] K. Popp and P. Stelter, Philos. Trans. R. Soc. London Ser. A **332**, 89 (1990).  
 [5] H. J. S. Feder and J. Feder, Phys. Rev. Lett. **66**, 2669 (1991), **67**, 283(E) (1991).  
 [6] T. Baumberger, F. Heslot, and B. Perrin, Nature **367**, 544 (1994).  
 [7] A. Johansen *et al.*, Phys. Rev. E **48**, 4779 (1993).  
 [8] H. Yoshizawa, P. McGuiggan, and J. Israelachvili, Science **259**, 1305 (1993).  
 [9] G. Reiter, L. Demirel, and S. Granick, Science **263**, 1741 (1994).  
 [10] J. M. Georges, S. Millot, J. L. Loubet, and A. Tonck, J. Chem. Phys. **98**, 7345 (1993).  
 [11] J. Klein and E. Kumacheva, Science **269**, 816 (1995).  
 [12] P. A. Thompson and M. O. Robbins, Science **250**, 792 (1990).  
 [13] P. A. Thompson, M. O. Robbins, and G. S. Grest, Isr. J. Chem. **35**, 93 (1995).  
 [14] M. O. Robbins, P. A. Thompson, and G. S. Grest, MRS Bull. **18**, 45 (1993).  
 [15] B. N. J. Persson, Phys. Rev. B **50**, 4771 (1994).  
 [16] Y. Braiman, F. Family, and G. Hentschel, Phys. Rev. E **53**, R3005 (1996).  
 [17] J. M. Carlson and A. A. Batista, Phys. Rev. E **53**, 4153 (1996).

- [18] B. N. J. Persson, *Chem. Phys. Lett.* **254**, 114 (1996).
- [19] P. Bak, C. Tang, and K. Wiesenfeld, *Phys. Rev. Lett.* **59**, 381 (1987).
- [20] F. J. Elmer, in *Physics of Sliding Friction*, edited by B. N. J. Persson and E. Tosatti (Kluwer, Dordrecht, 1996), pp. 433–447.
- [21] M. G. Rozman, M. Urbakh, and J. Klafter, *Phys. Rev. Lett.* **77**, 683 (1996).
- [22] F. J. Elmer, *Phys. Rev. E* **50**, 4470 (1994).
- [23] M. Weiss and F. J. Elmer, *Phys. Rev. B* **53**, 7539 (1996).
- [24] A. L. Demirel and S. Granick (unpublished).
- [25] G. M. Zaslavsky, *Chaos* **4**, 589 (1994).
- [26] D. F. Escande, *Phys. Rep.* **121**, 165 (1985).
- [27] B. P. Koch and R. W. Leven, *Physica D* **16**, 1 (1985).
- [28] In our earlier publication [21] we did not consider in detail the transition between stick-slip and kinetic regimes. Region (b) was not separated from (a).
- [29] H. D. I. Abarbanel, R. Brown, J. L. Sidorowich, and L. S. Tsimring, *Rev. Mod. Phys.* **65**, 1331 (1993).
- [30] H.-W. Hu, G. A. Carson, and S. Granick, *Phys. Rev. Lett.* **66**, 2758 (1991).
- [31] M. Urbakh, L. Daikhin, and J. Klafter, *J. Chem. Phys.* **103**, 10 707 (1995).
- [32] N. N. Bogoliubov and Y. A. Mitropolsky, *Asymptotic Methods in the Theory of Nonlinear Oscillations* (Gordon and Breach, New York, 1961).
- [33] S. H. Strogatz, *Nonlinear Dynamics and Chaos* (Addison-Wesley, Reading, MA, 1994).
- [34] A. Wolf, J. B. Swift, H. L. Swinney, and J. A. Vastano, *Physica D* **16**, 285 (1985).
- [35] G. Benettin, L. Galgani, A. Giorgilli, and J.-M. Strelcyn, *Mecanica* **15**, 9 (1980).
- [36] I. Shimada and T. Nagashima, *Prog. Theor. Phys.* **61**, 1605 (1979).
- [37] *Handbook of Mathematical Functions*, 8th ed., edited by M. Abramowitz (Dover, New York, 1972).